Guided wave propagation in cylindrical ducts with elastic walls enclosing a fluid moving with a uniform velocity.

Ray Kirby*

Centre for Audio, Acoustics and Vibration

University of Technology Sydney

Sydney, NSW, 2007

Australia

Wenbo Duan

Department of Mechanical, Aerospace and Civil Engineering

Brunel University London

Uxbridge

Middlesex

UB8 3PH

United Kingdom

*Corresponding Author

Abstract

Theoretical models for elastic wave propagation in fluid filled ducts normally neglects mean fluid flow. However, in many engineering applications the velocity of the fluid may influence the modal characteristics of the duct, for example in gas pipelines, turbomachinery applications and ventilation systems. Accordingly, the influence of a mean uniform fluid flow on acoustically driven duct wall vibration is analysed here for a cylindrical geometry. The semi-analytic finite element method is used to couple the elastodynamic wave equation for the duct wall to the convected wave equation for sound propagation in a uniform fluid flow. A one dimensional finite element approach is described and this is used to find the coupled eigenmodes for the duct. Under certain conditions, a uniform mean flow is seen to significantly affect the phase speed for different eigenmodes, and it is shown that this may cause energy to transfer from the fluid to the surrounding wall at frequencies much lower than those seen without mean flow. This behaviour has the potential to increase sound radiation from ducts at lower frequencies when mean flow is present.

Keywords: SAFE method, mean fluid flow, elastic walls, duct acoustics

1. Introduction

Noise propagation in ductwork is often generated by turbomachinery such as fans or turbines. The ductwork is designed to move air or expel exhaust gases, and so the noise generated by these machines is convected along the ductwork by a mean gas flow. In many engineering applications it is common for the velocity of the gas inside the duct to extend to Mach numbers of 0.3 and above, and this can significantly affect the acoustic performance of a system. For example, Kirby et al. [1] investigate the influence of a mean gas flow on the acoustic performance of dissipative silencers, and Choy and Huang [2] investigate the influence of mean flow on drumlike silencers. In turbofan applications, Mach numbers well above 0.3 are common and the review by Astley [3] describes the influence of mean flow on the acoustics of these large engineering systems. Thus, the convective effect of a mean gas flow can significantly alter the acoustic behaviour of many different engineering systems, although in duct acoustics investigations into the influence of mean flow have generally been restricted to controlling noise using devices such as silencers or duct liners. The influence of a mean gas flow on the vibro-acoustic behaviour of duct walls has largely been neglected, even though it is common for the sound field inside the duct to couple to the duct wall and drive the vibration of these walls. This generates noise that radiates away from the duct and is often referred to as breakout noise. This can contribute significantly to the overall noise levels radiated by a duct [4], and so it is important also to understand the influence of mean flow on the radiation characteristics of a duct. Accordingly, this article presents a numerical model that is suitable for predicting the influence of a fluid moving with a uniform velocity on the acoustically driven vibrations of a duct wall.

The analysis of acoustically driven duct wall vibrations presents a number of challenges, including coupling an appropriate representation of wave propagation in the duct wall to the wave equation in the fluid. The most popular methods for achieving this assume that the wall is either a membrane or an elastic plate described using a low frequency or thin wall/shell approximation. For example, Huang [4], Choy and Huang [2], and Lawrie and Guled [5] analyse membranes in ductwork using analytic [5] and numerical methods [2]. Lawrie [6] extends this approach to the analysis of elastic waves using the fourth order beam equation to characterise the structure. This enables an analytic solution to be developed and, through derivation of an appropriate orthogonality relation, it is shown that a scattering matrix can be obtained for a finite section of elastic plate in a two dimensional duct. This work extends the analytic and numerical methods developed previously by Fahy and Pretlove [7], and later by Cummings [8]. Cummings also analysed low order mode propagation and developed asymptotic expressions for rectangular ductwork [9], as well as developing numerical approaches for more complicated geometries [10]. Fahy and Fuller [11] also applied analytic techniques to a fluid filled pipe and they demonstrate how the energy in particular eigenmodes can transfer between the

fluid and the structure depending on the frequency of excitation and the modal characteristics of the coupled system. This transfer of energy was also observed by Lawrie [12].

Mean flow is known to change the modal properties of a coupled system and this can have an influence on the energy transfer between the fluid and the structure. For example, Choy and Huang [2] demonstrate the influence of a uniform mean flow on the characteristics of their membrane based drumlike silencer. However, very few articles examine the effects of mean flow on duct wall vibrations, with only the numerical approach of Kirby and Cummings [13], and the analytic methods of Martin [14] being relevant to this current study. Instead, the majority of investigations focus on the influence of mean flow on the vibro-acoustic behaviour of plates. See for example Abrahams [15], and later Sucheendran et al. [16], who focus on developing analytic expressions for the scattering from a finite elastic plate subjected to a grazing mean flow. Other applications include the analysis of blood flow by Klochkov [17], who used an analytic approach to examine a cylindrical structure with uniform mean flow. However, the methods developed in these different areas of application continue to assume low frequencies and/or thin plates, and Cummings [18] notes that this potentially limits the application of these approaches in many engineering problems in duct acoustics.

To remove the low frequency/thin wall approximation it is necessary to return to the elastodynamic wave equation. Application of this equation has seen favour in the area of structural health monitoring, where predictions are often required in the ultrasonic frequency range. Both analytic and numerical methods have been developed, see for example the commercial code DISPERSE®, which uses an analytic solution for the coupled problem [19]. More recently, alternative numerical approaches have been developed, including the wave finite element method [20], and the semi analytic finite element (SAFE) method [21]. These numerical models have been applied to liquid filled pipes and demonstrate that large numbers of eigenmodes can readily be obtained. However, these models have yet to be applied to ductwork applications, and they also neglect the effects of a mean fluid flow.

This article applies the SAFE method in the analysis of acoustically driven wall vibrations for a circular duct that includes a uniform mean flow. The aim of the article is to investigate the influence of mean flow on the modal characteristics of a duct, with a focus on investigating phenomena likely to affect the acoustic performance of ductwork used in ventilation and turbomachinery applications. The analysis is restricted to circular ducts as this simplifies the problem and enables a focus on modal behaviour. External fluid loading is also neglected, although this can be included if necessary, see for example Kalkowski et al. [21] and Duan et al. [22]. In this article, a uniform mean flow is assumed for the fluid as this is generally accepted to provide a good approximation in duct acoustics [1]; however, the numerical approach presented in the next section is sufficiently general to include shear layers if

desired, although the addition of viscosity will significantly complicate the finite element analysis for the acoustic wave equation. Accordingly, in section 2 a SAFE approach is developed to compute the coupled eigenmodes for uniform mean flow in an elastic circular duct; in section 3 dispersion curves are presented and the relevant modal characteristics examined; conclusions are drawn in section 4.

2. Theory

In this section an eigenproblem is derived for an infinite cylindrical duct, where the fluid inside the duct is denoted region Ω_0, and this is surrounded by a thick elastic wall, denoted region Ω_1, see Fig. 1. A cylindrical co-ordinate system (r, θ, z) is adopted, and the fluid inside the duct moves with a uniform velocity $\mathbf{v} = [0 \quad 0 \quad \mathrm{v}_z]$.

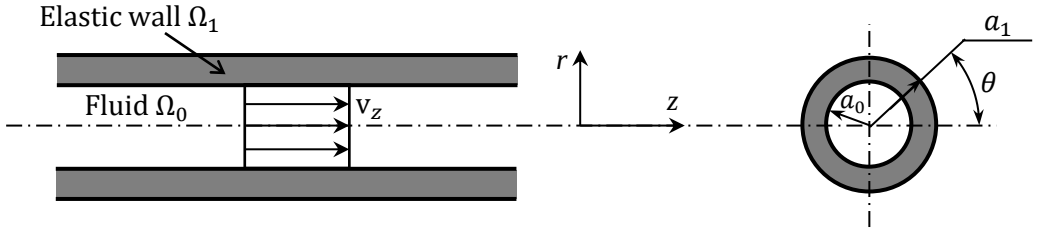

Figure 1. Geometry of fluid filled elastic duct.

The convected acoustic wave equation for the fluid in region Ω_0 is [23],

$$\nabla^2 p^* - \frac{1}{c_0^2}\left[\frac{\partial}{\partial t} + \mathbf{v}\cdot\nabla\right]^2 p^* = 0, \tag{1}$$

where, p^* is the acoustic pressure in the fluid, c_0 is the speed of sound in the fluid, and t is time. The elastodynamic wave equation for the [thick] duct wall in region Ω_1 is [24],

$$\nabla\cdot\boldsymbol{\sigma} = \rho\frac{\partial^2 \mathbf{u}^*}{\partial t^2}, \tag{2}$$

where $\boldsymbol{\sigma}$ is the Cauchy stress tensor, ρ is the duct wall density, and $\mathbf{u}^* = [u_r^* \quad u_\theta^* \quad u_z^*]$ is the duct wall displacement. An eigenproblem is obtained by expanding the wall displacement and acoustic pressure over an infinite set of eigenmodes, so that

$$\mathbf{u}^*(r,\theta,z;t) = \sum_{m=0}^{\infty}\sum_{n=0}^{\infty}\mathbf{u}_m(r)e^{i[\omega t - n\theta - k_T\gamma_m z]}, \tag{3}$$

and

$$\mathrm{p}^*(r,\theta,z;t) = \sum_{m=0}^{\infty}\sum_{n=0}^{\infty} \mathrm{p}_m(r) e^{i[\omega t - n\theta - k_T \gamma_m z]}. \tag{4}$$

Here, ω is the radian frequency, $i = \sqrt{-1}$, γ is the coupled wavenumber and $k_T = \omega/c_T$, where c_T is the shear (or torsional) bulk wave velocity in the duct wall.

The governing wave equation for the structure is separated into three scalar equations using the usual expansions for the Cauchy stress tensor in cylindrical coordinates [24]. The modal expansions in Eqs. (3) and (4) are then substituted into the relevant equation, and a weighted residual formulation is applied [25]. This involves weighting the three scalar equations for the structure using the arbitrary function w_q, where $q = r, \theta \; or \; z$, respectively, and for the fluid the weighting function w_0 is chosen. This yields four equations for modes m and n:

$$\int_{a_0}^{a_1} \left\{ \sigma_{rr} \frac{\partial w_r}{\partial r} + \frac{in}{r} w_r \sigma_{r\theta} + i k_T \gamma_m w_r \sigma_{rz} - \frac{w_r}{r}[\sigma_{rr} - \sigma_{\theta\theta}] - \rho\omega^2 w_r u_r \right\} r dr = [w_r \sigma_{rr} n_r]_{a_0}^{a_1}, \tag{5}$$

$$\int_{a_0}^{a_1} \left\{ \sigma_{\theta r} \frac{\partial w_\theta}{\partial r} + \frac{in}{r} w_\theta \sigma_{\theta\theta} + i k_T \gamma_m w_\theta \sigma_{\theta z} - \frac{2w_\theta}{r} \sigma_{r\theta} - \rho\omega^2 w_\theta u_\theta \right\} r dr = [w_\theta \sigma_{\theta r} n_r]_{a_0}^{a_1}, \tag{6}$$

$$\int_{a_0}^{a_1} \left\{ \sigma_{zr} \frac{\partial w_z}{\partial r} + \frac{in}{r} w_z \sigma_{z\theta} + i k_T \gamma_m w_z \sigma_{zz} - \frac{w_z}{r} \sigma_{rz} - \rho\omega^2 w_z u_z \right\} r dr = [w_z \sigma_{zr} n_r]_{a_0}^{a_1}, \tag{7}$$

$$\int_{0}^{a_0} \left\{ \frac{\partial w_0}{\partial r}\frac{\partial p}{\partial r} - \frac{w_0}{r}\frac{\partial p}{\partial r} + \frac{n^2}{r^2} w_0 p - 2\mathrm{M} k_0 k_T \gamma_m w_0 p + [1 - \mathrm{M}^2] k_T^2 \gamma_m^2 w_0 p - k_0^2 w_0 p \right\} = \left[w_0 \frac{\partial p}{\partial r} n_r \right]_0^{a_0}. \tag{8}$$

Here, $k_0 = \omega/c_0$, the Mach number $\mathrm{M} = \mathrm{v}_z/c_0$, and n_r is the outwards unit normal in the r direction. These four equations are solved using a finite element discretisation, so that the wall displacement and the pressure in the fluid are discretised to give $\mathrm{u}_q = \mathbf{N}_q \mathbf{u}_q$ and $p = \mathbf{N}\mathbf{p}$, where $q = r, \theta \; or \; z$, and $\mathbf{N}$ is the global shape function for the finite element mesh [25]. Adopting isoparametric elements [25], yields the following four equations:

$$\mathbf{R}_{10}\tilde{\mathbf{u}}_r - \zeta^2\mathbf{R}_{12}\tilde{\mathbf{u}}_r + \mathbf{\Theta}_{10}\tilde{\mathbf{u}}_\theta + \zeta\mathbf{Z}_{11}\tilde{\mathbf{u}}_z = \frac{1}{\mu}[w_r\sigma_{rr}n_r]_{a_0}^{a_1}, \tag{9}$$

$$\mathbf{\Theta}_{20}\tilde{\mathbf{u}}_\theta - \zeta^2\mathbf{\Theta}_{22}\tilde{\mathbf{u}}_\theta + \mathbf{R}_{20}\tilde{\mathbf{u}}_r + \zeta\mathbf{Z}_{21}\tilde{\mathbf{u}}_z = \frac{1}{\mu}[w_\theta\sigma_{\theta r}n_r]_{a_0}^{a_1}, \tag{10}$$

$$\mathbf{Z}_{30}\tilde{\mathbf{u}}_z - \zeta^2\mathbf{Z}_{32}\tilde{\mathbf{u}}_z + \zeta\mathbf{R}_{31}\tilde{\mathbf{u}}_r + \zeta\mathbf{\Theta}_{31}\tilde{\mathbf{u}}_\theta = \frac{1}{\mu}[w_z\sigma_{zr}n_r]_{a_0}^{a_1}. \tag{11}$$

The matrices in each equation are given in the Appendix, and $\zeta = ik_T\gamma$. In addition, the displacement has been normalised so that $a_0\tilde{\mathbf{u}} = [u_r \quad iu_\theta \quad u_z]$. Similarly, for the fluid

$$\mathbf{R}_{00}\tilde{\mathbf{p}} + \zeta\mathbf{R}_{01}\tilde{\mathbf{p}} - \zeta^2\mathbf{R}_{02}\tilde{\mathbf{p}} = \frac{1}{a_0\rho_0\omega^2}\left[w_0\frac{\partial p}{\partial r}n_r\right]_0^{a_0}, \tag{12}$$

where $a_0^2\rho_0\omega^2\tilde{\mathbf{p}} = \mathbf{p}$, and ρ_0 is the density of the fluid.

The boundary conditions for each region are now applied. For the fluid, $\partial p/\partial r|_{r=0} = 0$, and for the pipe wall,

$$\sigma_{rr}|_{r=a_1} = \sigma_{\theta r}|_{r=a_0} = \sigma_{\theta r}|_{r=a_1} = \sigma_{zr}|_{r=a_0} = \sigma_{zr}|_{r=a_1} = 0. \tag{13}$$

At the interface between the fluid and the structure, continuity of displacement in the radial direction is applied [1, 2], so that

$$\frac{\partial p}{\partial r} = \rho_0\omega^2\left[1 + i\frac{\zeta\mathrm{M}}{k_0}\right]^2 u_r, \tag{14}$$

and continuity of pressure/stress [21], so that

$$p = -\sigma_{rr}. \tag{15}$$

Substitution of these boundary conditions back into equations (9) and (12) yields the following

$$\mathbf{R}_{10}\tilde{\mathbf{u}}_r - \zeta^2\mathbf{R}_{12}\tilde{\mathbf{u}}_r + \mathbf{\Theta}_{10}\tilde{\mathbf{u}}_\theta + \zeta\mathbf{Z}_{11}\tilde{\mathbf{u}}_z - \frac{\rho_0}{\rho_1}a_0^2k_T^2\mathbf{W}_r^T\mathbf{N}_f\tilde{\mathbf{p}}\big|_{r=a_0} = 0, \tag{16}$$

and

$$\mathbf{R}_{00}\tilde{\mathbf{p}} + \zeta\mathbf{R}_{01}\tilde{\mathbf{p}} - \zeta^2\mathbf{R}_{02}\tilde{\mathbf{p}} - \left[1 + 2i\frac{\zeta \mathrm{M}}{k_0} - \frac{\zeta^2 \mathrm{M}^2}{k_0^2}\right]\mathbf{W}_0^{\mathrm{T}}\mathbf{N}\tilde{\mathbf{u}}_r\big|_{r=a_0} = 0. \tag{17}$$

Equations (10) and (11), with the relevant boundary conditions from (13) added, are combined with Eqs. (16) and (17) to given the final eigenequation:

$$\begin{bmatrix}\mathbf{0} & \mathbf{X}^{\mathbf{T}} \\ \mathbf{X} & \mathbf{Y}\end{bmatrix}\begin{Bmatrix}\mathbf{L} \\ \zeta\mathbf{L}\end{Bmatrix} = \zeta\begin{bmatrix}\mathbf{X}^{\mathbf{T}} & \mathbf{0} \\ \mathbf{0} & \mathbf{Z}\end{bmatrix}\begin{Bmatrix}\mathbf{L} \\ \zeta\mathbf{L}\end{Bmatrix}, \tag{18}$$

where, $\mathbf{L} = [\tilde{\mathbf{p}} \quad \tilde{\mathbf{u}}_r \quad \tilde{\mathbf{u}}_\theta \quad \tilde{\mathbf{u}}_z]$ and

$$\mathbf{X} = \begin{bmatrix}\mathbf{R}_{00} & -\mathbf{C}_{01} & \mathbf{0} & \mathbf{0} \\ -\mathbf{C}_{10} & \mathbf{R}_{10} & \mathbf{\Theta}_{10} & \mathbf{0} \\ \mathbf{0} & \mathbf{R}_{20} & \mathbf{\Theta}_{20} & \mathbf{0} \\ \mathbf{0} & \mathbf{0} & \mathbf{0} & \mathbf{Z}_{30}\end{bmatrix}, \qquad \mathbf{Y} = \begin{bmatrix}\mathbf{R}_{01} & -\mathbf{C}_{11} & \mathbf{0} & \mathbf{0} \\ \mathbf{0} & \mathbf{0} & \mathbf{0} & \mathbf{Z}_{11} \\ \mathbf{0} & \mathbf{0} & \mathbf{0} & \mathbf{Z}_{21} \\ \mathbf{0} & \mathbf{R}_{31} & \mathbf{\Theta}_{31} & \mathbf{0}\end{bmatrix}, \tag{19, 20}$$

and

$$\mathbf{Z} = \begin{bmatrix}\mathbf{R}_{02} & -\mathbf{C}_{21} & \mathbf{0} & \mathbf{0} \\ \mathbf{0} & \mathbf{R}_{12} & \mathbf{0} & \mathbf{0} \\ \mathbf{0} & \mathbf{0} & \mathbf{\Theta}_{22} & \mathbf{0} \\ \mathbf{0} & \mathbf{0} & \mathbf{0} & \mathbf{Z}_{32}\end{bmatrix}. \tag{21}$$

The coupling matrices are given as

$$\mathbf{C}_{01} = \mathbf{W}_0^{\mathrm{T}}\mathbf{N}|_{r=a_0}, \qquad \mathbf{C}_{10} = \frac{\rho_0}{\rho_1}a_0^2k_T^2\mathbf{W}_r^T\mathbf{N}_f\Big|_{r=a_0}, \tag{22, 23}$$

and

$$\mathbf{C}_{11} = 2i\left(\frac{\mathrm{M}}{k_0}\right)\mathbf{W}_0^{\mathrm{T}}\mathbf{N}|_{r=a_0}, \qquad \mathbf{C}_{21} = \left(\frac{\mathrm{M}}{k_0}\right)^2\mathbf{W}_0^{\mathrm{T}}\mathbf{N}|_{r=a_0}. \tag{24, 25}$$

Equation (18) is an eigenequation of order of $N_t = 2(N_p + 3N_u)$, where N_p is the number of nodes in the fluid, and N_u is the total number of nodes in the duct wall. On solution of this eigenequation, the phase velocity c_p for mode m is given as

$$\mathrm{c}_p = \frac{\omega}{\mathrm{Re}(-i\zeta)}. \tag{26}$$

3. Results and Discussion

Dispersion curves are presented in this section for two example problems that are designed to illustrate the influence of mean flow. The parameters used in each example are listed below in Table 1, and other relevant parameters, such as the Lamé constants, can be found from the usual relationships [26].

Table 1
Parameters for numerical experiments

Duct	a_0 (m)	a_1 (m)	ρ_0 (kg/m^3)	c_0 (m/s)	ρ (kg/m^3)	E (N/m^2)	ν
A	0.160	0.180	1.204	344.224	1100	2.3×10^9	0.400
B	1.200	1.210	1.204	344.224	7830	2.14×10^{11}	0.287

All of the solutions presented below have been computed using 16 quadratic line elements in the fluid and 6 in the structure, which gives $N_t = 144$. This number of elements have been chosen to ensure convergence to at least two decimal places for the phase velocities shown in the figures that follow; a more detailed discussion on the convergence of the one dimensional SAFE method can be found in Duan et al. [22].

The results presented in this section are restricted to axisymmetric modes, so that in the solution of Eq. (18), $n = 0$. Moreover, the aim of this article is to examine the influence of mean flow on coupled wave propagation and so it is appropriate to start by examining dispersion curves without mean flow in order to provide a benchmark comparison. Accordingly, in Fig. 2 the phase velocity is plotted for duct A without mean flow. The phase velocity is normalised here against c_0 so that one can clearly identify the fundamental fluid mode in the duct (which is the acoustic plane wave with $c_p = c_0$ when the duct walls are rigid). The excitation frequency is normalised against the ring frequency f_{ring}, which is defined here as $f_{\text{ring}} = c_L/\pi(a_0 + a_1)$, where c_L is the compressional (or longitudinal) bulk wave velocity in the duct wall.

In Fig. 2 it is seen that for this geometry a complicated set of dispersion curves are present and so in order to provide clarity for these diagrams, as well as those that follow, the shear (or torsional) modes propagating in the structure have been omitted as these do not couple to the fluid. It is evident that the first two axisymmetric compressional (or longitudinal) modes propagate across the entire frequency range, and at low frequencies acoustic energy lies either in the fluid (a fluid type mode), or the structure (a structural type mode). As the frequency is increased, additional higher order axisymmetric longitudinal modes begin to propagate. These modes can be identified as either structural or fluid type modes by overlaying the uncoupled structural modes.

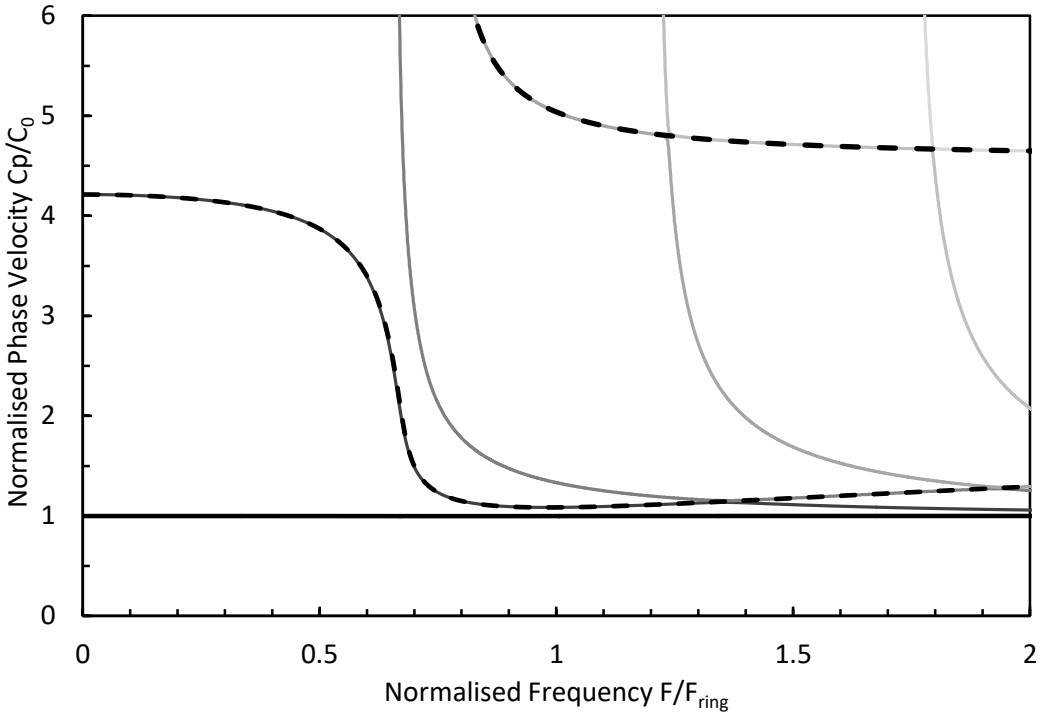

Figure 2. Normalised phase velocity for duct A, with $\mathrm{M} = 0$. ——— , coupled fluid type mode; ——— , coupled higher order compressional modes; – – – , uncoupled compressional modes for the structure only.

It is evident in Fig. 2 that when $\mathrm{M} = 0$ the coupling between the fluid and the wall for the fundamental fluid type mode is weak, so that the phase velocity remains close to that of a plane wave in a rigid duct ($c_p/c_0 = 1$). However, for the higher order modes a more complicated picture emerges. For example, modes are seen to transfer their energy from the structure to the fluid, and vice versa, as the frequency is increased. This illustrates the complexity of this type of coupled guided wave problem and this is behaviour that has been shown before [13]. Of course, it is also well known that the compressional modes never cross one another in the dispersion curves of a lossless system, and instead they avoid crossing, or veer apart, as the energy is transferred between the fluid and the structure [12, 21].

In Fig. 3, mean flow is now added to the same problem as that studied in Fig. 2. It is clear in Fig. 3 that for the parameters chosen here the addition of mean flow has significantly altered the behaviour of the fundamental fluid type mode. This change in behaviour has occurred because of the convective effect of the mean fluid flow, which is seen to cause energy to transfer from the fundamental fluid type mode into the structure at a frequency below the ring frequency of the duct.

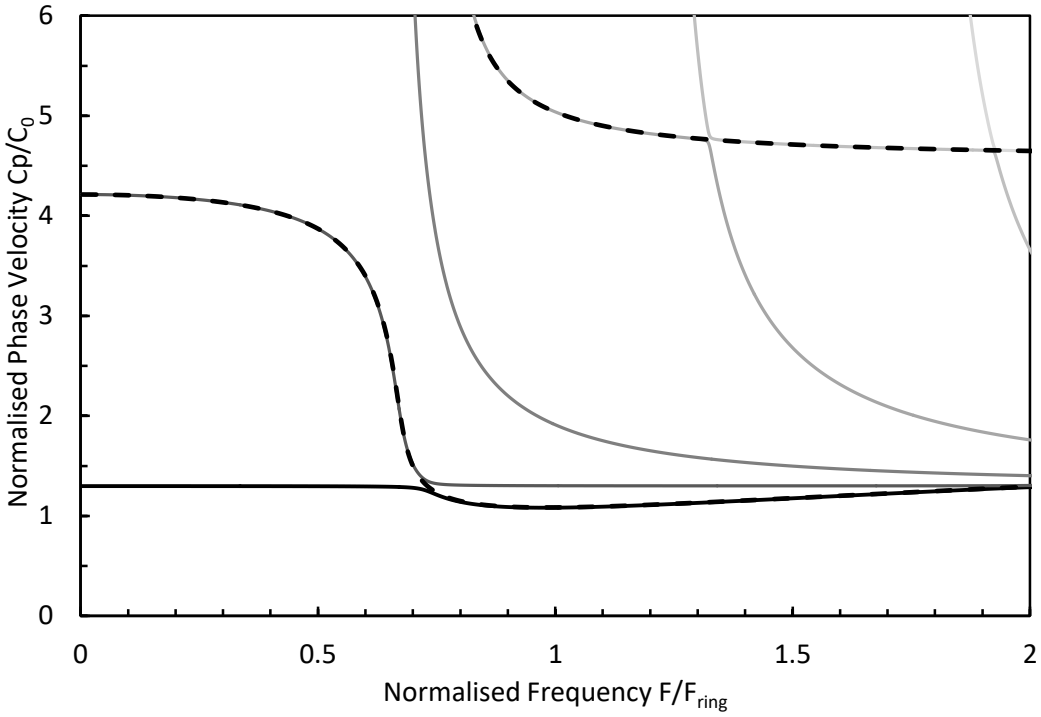

Figure 3. Normalised phase velocity for duct A, with $\mathrm{M} = 0.3$. ——— , coupled fluid type mode;
———, coupled higher order compressional modes;
– – – , uncoupled compressional modes for the structure only.

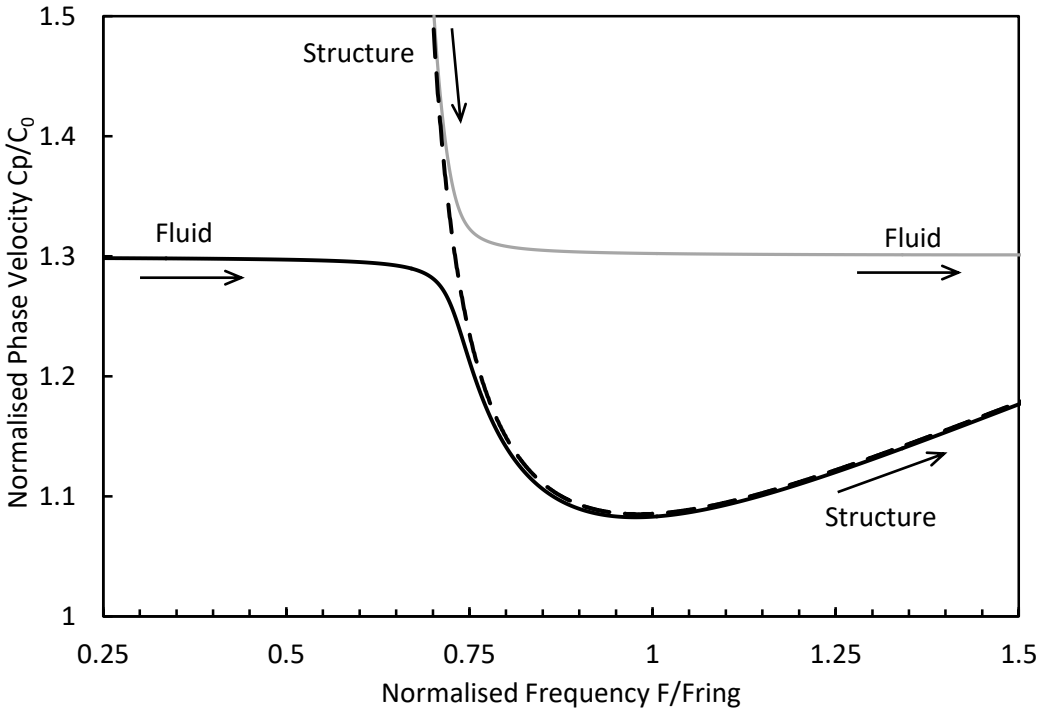

Figure 4. Transfer of energy between the fluid and structure
at an avoided crossing for duct A, with M=0.3.

The behaviour in Fig. 3 is more clearly observed in Fig. 4, where the dispersion curve is magnified. One can observe the veering phenomenon more closely, as the fundamental fluid type mode approaches a structural type mode but avoids crossing and so the energy transfers from the fluid to the structure. The change in behaviour observed in Figs. 3 and 4 has been caused by the convective effect of the mean flow and this has potential implications for engineering applications. For example, at low frequencies acoustic energy normally resides in the fundamental fluid type mode for turbomachinery applications. The presence of mean flow in this example causes this energy to transfer from the fluid to the structure below the ring frequency and this may cause an increase in the radiated sound power at lower frequencies.

In Fig. 5, a larger duct is studied as this illustrates a problem in which a much larger number of modes propagate. Figure 5 omits mean flow and here one can see a large number of fluid type modes propagating, which then transfer their energy into structural type modes. In this problem, these modes are seen to swap energy between the structure and the fluid a number of times depending on the excitation frequency. This behaviour is illustrated in Fig. 5 using alternate dashed and solid lines in order to better illustrate this behaviour. Note that for this combination of frequency range and material parameters, the fundamental fluid type mode again remains only very weakly coupled to the structure.

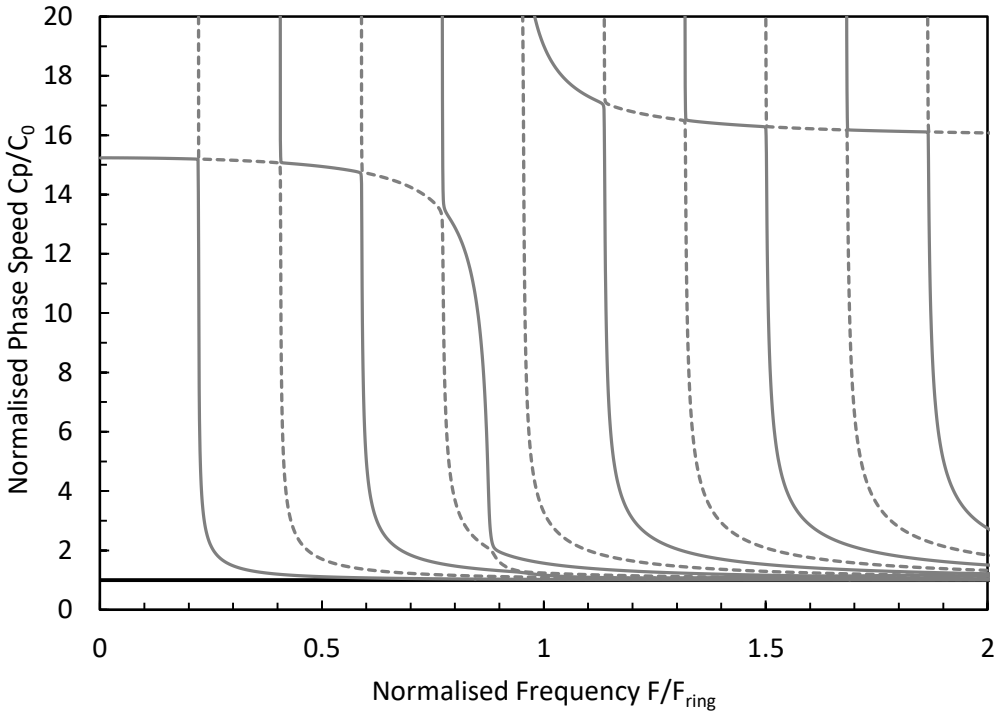

Figure 5. Normalised phase velocity for duct B, with $\mathrm{M} = 0$. ——, coupled fluid type mode; ——, - - - - coupled higher order compressional modes.

In Fig. 6 mean flow is added and the veering behaviour observed previously is also seen to occur for duct B. This is again illustrated more clearly by the magnified version in Fig. 7. This further illustrates the influence of mean flow on this veering phenomenon, and a very significant impact on the phase speed is observed for the fundamental fluid type mode. It is interesting also to note that for this larger duct mean flow also changes the phase speed of the coupled higher order modes. This behaviour is potentially important in the study of sound propagation in larger ductwork. For example, it is common for sound sources such as fans or turbines to excite higher order acoustic modes in a duct [27]. This means that the sound radiated by the walls of a duct will depend on the energy transfer between the sound source and these higher order modes (as well as the fundamental mode). Figure 7 illustrates that this energy transfer will be affected by the presence of mean flow, so that mean flow has the potential to change the noise radiation characteristics of a duct in which noise is generated by turbomachinery.

Finally, it is noted that the modal solutions obtained when mean flow was present did not show any evidence of the numerical instabilities described recently by Martin [15]. Martin investigated the kinematic radial boundary conditions of continuity of velocity and displacement, which was motivated by concern over the stability of solutions obtained when coupling mean fluid flow to an approximate form of the wave equation for a plate. Martin concluded that displacement was the more suitable boundary condition, although it was suggested that a “deeper numerical analysis is necessary”. Furthermore, concerns surrounding the stability of the displacement boundary condition have also been expressed when coupling a uniform mean flow to ducts with a locally reacting surface [28]. However, in this investigation continuity of displacement was seen to be stable for a large range of parameters (not shown in this article) and so no evidence was found to support the use of an alternative boundary condition.

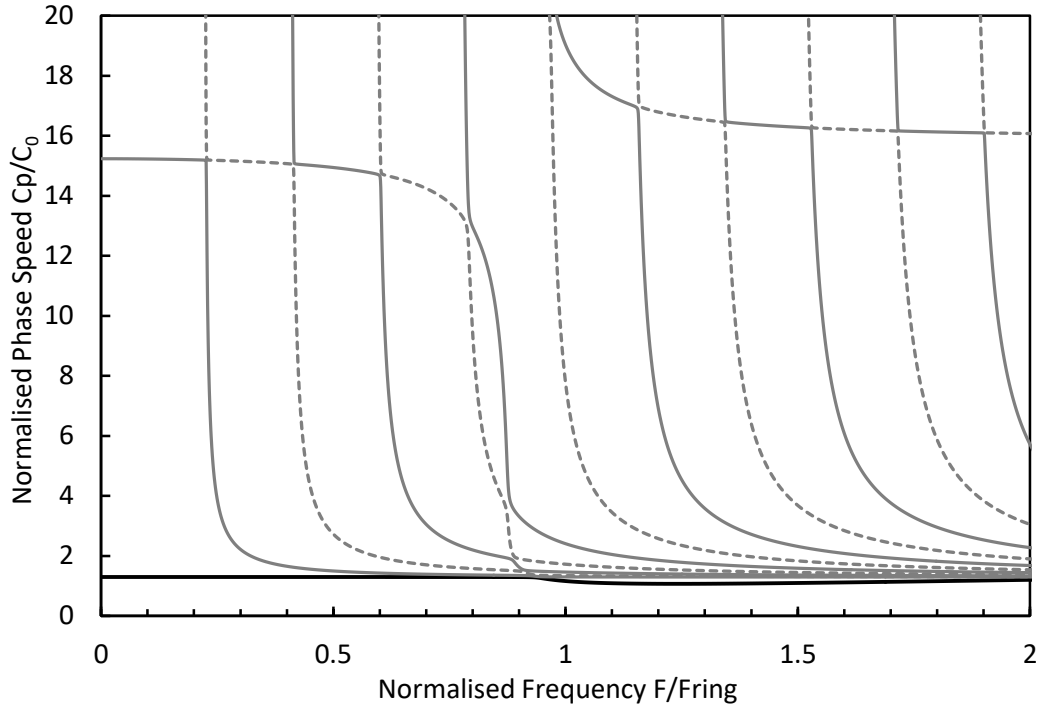

Figure 6. Normalised phase velocity for duct B, with $M = 0.3$. ——— , coupled fluid type mode; ———, - - - - - coupled higher order compressional modes.

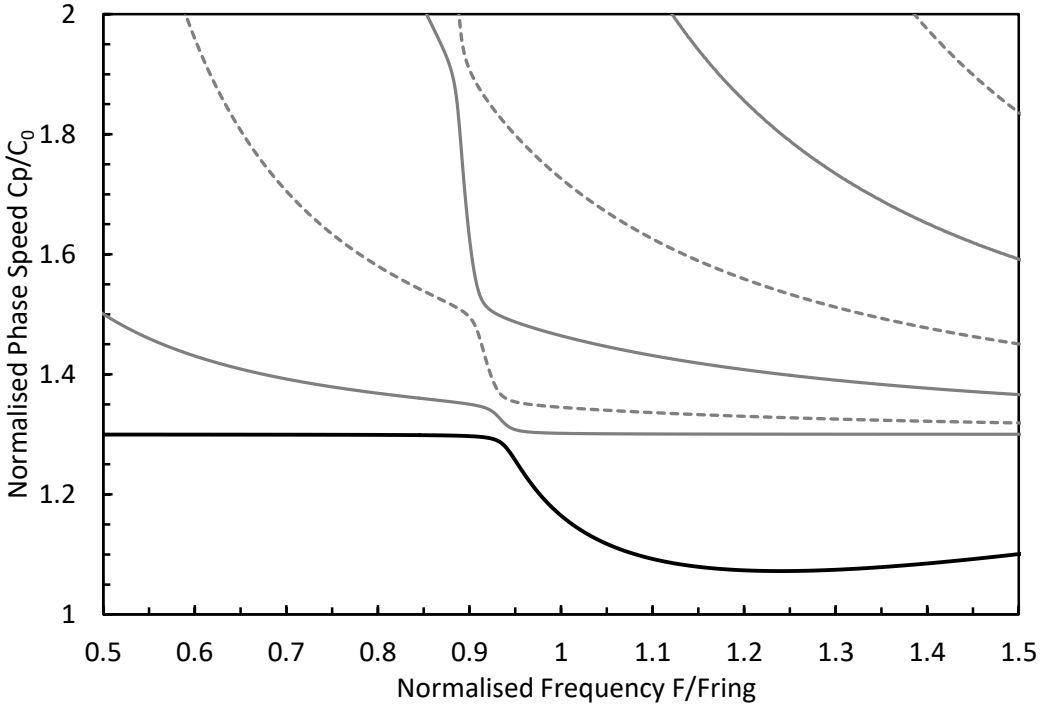

Figure 7. Transfer of energy between the fluid and structure
at an avoided crossing for duct B, with M=0.3.

4. Conclusions

This article presents a SAFE approach to obtaining the eigenmodes for acoustically driven wall vibration in circular ductwork. The SAFE method facilities the addition of uniform mean flow in the interior of the duct, and the sound pressure field in the fluid is coupled to the wall displacement using continuity of displacement as the kinematic radial boundary condition. Predictions are presented for two sample problems and the phase velocities are compared with and without mean flow. In both cases the phenomenon of energy transfer between the fluid and the structure is observed as the excitation frequency is increased. The addition of mean flow is seen to significantly change the characteristics of this energy transfer, when compared to the no flow case, at least for the example problems studied here.

The addition of mean flow is seen to transfer energy from the fundamental fluid type mode to the structure at frequencies much lower than those observed in the absence of flow. This has potential ramifications for turbomachinery applications, as the acoustic energy is predominantly carried by the fluid at lower frequencies. Accordingly, it is possible for the mean flow to significantly change the noise radiation characteristics of ductwork used in turbomachinery applications, and for energy to transfer from the fluid to the structure at much lower frequencies than normally expected. This may lead to unexpected break-out noise problems occurring, especially if the initial design work was undertaken in the absence of mean flow.

The results presented in this article are intended to illustrate the potential change in behaviour that may be encountered under particular conditions within engineering ductwork. However it is recognised that the parameters chosen here indicate that this behaviour is likely to be relevant to more extreme engineering applications, such as the control of noise emitted by gas turbine exhaust systems. Nevertheless, this article presents a method for including uniform mean flow in the analysis of acoustically driven wall vibrations in circular ducts. The use of a finite element based approach also means that the method can readily be extended to rectangular and irregular cross-sectional geometries. Furthermore, in the future the authors aim to add in fluid viscosity so that shear layers may be included and a wider range of applications may be considered.

Appendix A

The matrices that make up the governing eigenequation are as follows:

$$\mathbf{R}_{00} = [\mathbf{K}_0 - \mathbf{K}_{02} + n^2\mathbf{M}_{02} - k_0^2]; \quad \mathbf{R}_{01} = 2i\mathrm{M}k_0\mathbf{M}_0; \quad \mathbf{R}_{02} = (1-\mathrm{M}^2)\mathbf{M}_0. \qquad \text{(A1, A2, A3)}$$

$$\mathbf{R}_{10} = \mathbf{K}_1 - 2\mathbf{K}_2 + \mathbf{K}_3 + (n^2+2)\mathbf{M}_2 - \mathbf{M}_7, \qquad \mathbf{R}_{12} = \mathbf{M}_1 \qquad \text{(A4, A5)}$$

$$\mathbf{\Theta}_{10} = n[\mathbf{K}_2 - \mathbf{K}_3 - 3\mathbf{M}_2], \text{ and } \mathbf{Z}_{11} = [\mathbf{K}_4 - \mathbf{K}_5] \qquad \text{(A6, A7)}$$

$$\mathbf{\Theta}_{20} = -\mathbf{K}_6 + 2\mathbf{K}_2 + \mathbf{K}_2^{\mathrm{T}} - n^2\mathbf{M}_3 - 2\mathbf{M}_2 + \mathbf{M}_7, \text{ and } \mathbf{\Theta}_{22} = -\mathbf{M}_1 \qquad \text{(A8)}$$

$$\mathbf{R}_{20} = n[\mathbf{K}_3^{\mathrm{T}} - \mathbf{K}_2^{\mathrm{T}} + \mathbf{M}_4], \text{ and } \mathbf{Z}_{21} = -n\mathbf{M}_5 \qquad \text{(A9, A10)}$$

$$\mathbf{Z}_{30} = \mathbf{K}_6 - \mathbf{K}_2 + n^2\mathbf{M}_2 - \mathbf{M}_7, \text{ and } \mathbf{Z}_{32} = \mathbf{M}_6 \qquad \text{(A11, A12)}$$

$$\mathbf{R}_{31} = \left[\mathbf{K}_5^{\mathrm{T}} - \mathbf{K}_4^{\mathrm{T}} + \mathbf{M}_5\right], \text{ and } \mathbf{\Theta}_{31} = -n\mathbf{M}_5 \qquad \text{(A13, A14)}$$

The matrices that make up these equations (where λ and μ are the Lamé constants) are:

$$\mathbf{K}_0 = a_0\int_0^{a_0}\frac{\partial\mathbf{w}_0^{\mathrm{T}}}{\partial r}\frac{\partial\mathbf{N}_0}{\partial r}r\,dr, \quad \mathbf{K}_{02} = a_0\int_0^{a_0}\mathbf{w}_0^{\mathrm{T}}\frac{\partial\mathbf{N}_0}{\partial r}\,dr \qquad \text{(A15, A16)}$$

$$\mathbf{K}_1 = a_0(\lambda+2\mu)\int_{a_0}^{a_1}\frac{\partial\mathbf{w}^{\mathrm{T}}}{\partial r}\frac{\partial\mathbf{N}}{\partial r}r\,dr, \quad \mathbf{K}_2 = a_0\mu\int_{a_0}^{a_1}\mathbf{w}^{\mathrm{T}}\frac{\partial\mathbf{N}}{\partial r}\,dr \qquad \text{(A17, A18)}$$

$$\mathbf{K}_3 = a_0\lambda\int_{a_0}^{a_1}\frac{\partial\mathbf{w}^{\mathrm{T}}}{\partial r}\mathbf{N}\,dr, \quad \mathbf{K}_4 = a_0\mu\int_{a_0}^{a_1}\mathbf{w}^{\mathrm{T}}\frac{\partial\mathbf{N}}{\partial r}r\,dr \qquad \text{(A19, A20)}$$

$$\mathbf{K}_5 = a_0\lambda\int_{a_0}^{a_1}\frac{\partial\mathbf{w}^{\mathrm{T}}}{\partial r}\mathbf{N}r\,dr, \quad \mathbf{K}_6 = a_0\mu\int_{a_0}^{a_1}\frac{\partial\mathbf{w}^{\mathrm{T}}}{\partial r}\frac{\partial\mathbf{N}}{\partial r}r\,dr \qquad \text{(A21, A22)}$$

$$\mathbf{M}_0 = a_0\int_0^{a_0}\mathbf{w}_0^{\mathrm{T}}\mathbf{N}_0 r\,dr, \quad \mathbf{M}_{02} = a_0\int_0^{a_0}\frac{1}{r}\mathbf{w}_0^{\mathrm{T}}\mathbf{N}_0\,dr \qquad \text{(A21, A22)}$$

$$\mathbf{M}_1 = a_0\mu\int_{a_0}^{a_1}\mathbf{w}^{\mathrm{T}}\mathbf{N}r\,dr, \quad \mathbf{M}_2 = a_0\mu\int_{a_0}^{a_1}\frac{1}{r}\mathbf{w}^{\mathrm{T}}\mathbf{N}\,dr \qquad \text{(A21, A22)}$$

$$\mathbf{M}_3 = a_0(\lambda+2\mu)\int_{a_0}^{a_1}\frac{1}{r}\mathbf{w}^{\mathrm{T}}\mathbf{N}\,dr, \quad \mathbf{M}_4 = a_0(\lambda+4\mu)\int_{a_0}^{a_1}\frac{1}{r}\mathbf{w}^{\mathrm{T}}\mathbf{N}\,dr \qquad \text{(A21, A22)}$$

$$\mathbf{M}_5 = a_0(\lambda+\mu)\int_{a_0}^{a_1}\mathbf{w}^{\mathrm{T}}\mathbf{N}dr, \quad \mathbf{M}_6 = a_0(\lambda+2\mu)\int_{a_0}^{a_1}\mathbf{w}^{\mathrm{T}}\mathbf{N}rdr \qquad \text{(A21, A22)}$$

$$\mathbf{M}_7 = a_0\mu k_T^2\int_{a_0}^{a_1}\mathbf{w}^{\mathrm{T}}\boldsymbol{N}rdr \qquad \text{(A21, A22)}$$

References

[1] R. Kirby, K. Amott, P.T. Williams, W. Duan, On the acoustic performance of rectangular splitter silencers in the presence of mean flow, Journal of Sound and Vibration 333 (2014) 6295-6311.

[2] Y.S. Choy, L. Huang, Effect of flow on the drumlike silencer, Journal of the Acoustical Society of America 118 (2005) 2077-3085.

[3] R.J. Astley, Numerical methods for noise propagation in moving flows, with application to turbofan engines, Acoustical Science and Technology 30 (2009) 227-239.

[4] L. Huang, A theoretical study of duct noise control by flexible panels, Journal of the Acoustical Society of America 106 (1999) 1801-1809.

[5] J.B. Lawrie and I.M.M. Guled, On tuning a reactive silencer by varying the position of an internal membrane, Journal of the Acoustical Society of America 120 (2006) 780-790.

[6] J.B. Lawrie, Analytic mode-matching for acoustic scattering in three dimensional waveguides with flexible walls: Application to a triangular duct, Wave Motion 50 (2013) 542-557.

[7] F. J. Fahy, A.J. Pretlove, Acoustic forces on a flexible panel which is part of a duct carrying airflow, Journal of Sound and Vibration 5 (1967) 302–316.

[8] A. Cummings, Sound transmission through duct walls, Journal of Sound and Vibration 239 (2001) 731-765.

[9] A. Cummings, The attenuation of sound in unlined ducts with flexible walls, Journal of Sound and Vibration 174 (1994) 433–450.

[10] A. Cummings, Approximate asymptotic solutions for acoustic transmission through the walls of rectangular ducts, Journal of Sound and Vibration 90 (1983) 211–227.

[11] A. Cummings, R.J. Astley, The effects of flanking transmission on sound attenuation in lined ducts, Journal of Sound and Vibration 179 (1995) 617–646.

[12] C.R. Fuller, F.J. Fahy, Characteristics of wave propagation and energy distributions in cylindrical elastic shells filled with fluid, Journal of Sound and Vibration 81 (1982) 501-518.

[13] J.B. Lawrie, M. Afzal, Acoustic scattering in a waveguide with a height discontinuity bridged by a membrane: a tailored Galerkin approach, Journal of Engineering Mathematics 105 (2017) 99-115.

[14] R. Kirby, A. Cummings, Structural/acoustic interaction in air-conditioning ducts in the presence of mean flow, Proceedings of ISMA 23 (1998) 677-684.

[15] V. Martin, Guided and convected acoustic wave coupled with vibrating walls: what kind of coupling? Proceedings of ICSV 24 (2017).

[16] I.D. Abrahams, Scattering of sound by an elastic plate with flow, Journal of Sound and Vibration, 89 (1983) 213-231.

[17] M. Sucheendran, D. Bodony, P. Guebelle, Coupled structural-acoustic response of a duct-mounted elastic plate with grazing flow, AIAA Journal, 52 (2014) 178-194.

[18] B.N. Klochkov, Wave effects in collapsible biovessels, Journal of Applied Mechanics and Technical Physics 56 (2015) 391-398.

[19] C. Aristégui, M.J.S. Lowe, P. Cawley, Guided waves in fluid-filled pipes surrounded by different fluids, Ultrasonics 39 (2001) 367-375.

[20] J.M. Renno, B.R. Mace, Vibration modelling of structural networks using a hybrid finite element/wave and finite element approach, Wave Motion 51 (2014) 566-580.

[21] M.K. Kalkowski, M.J. Muggleton, E. Rustighi, Axisymmetric semi-analytical finite elements for modelling waves in buried/submerged fluid-filled waveguides, Computers and Structures 196 (2018) 327-340.

[22] W. Duan, R. Kirby, P. Mudge, T-H. Gan, A one dimensional numerical approach for computing the eigenmodes of elastic waves in buried pipelines, Journal of Sound and Vibration 384 (2016) 177-193.

[23] A.D. Pierce, Wave equation for sound in fluids with unsteady inhomogeneous flow, Journal of the Acoustical Society of America 87 (1990) 2292-2299.

[24] W.S. Slaughter, The Linearized Theory of Elasticity, 1st Ed., Springer, Boston (2002).

[25] W.B. Bickford, A First Course in the Finite Element Method, 2nd Ed., Irwin, Boston (1994).

[26] J.D. Achenbach, *Wave Propagation in Elastic Solids*, 8th Ed., Elsevier, Amsterdam (1999).

[27] F.P. Mechel, Theory of baffle-type silencers, Acustica 70 (1990) 93-111.

[28] Y. Renou, Y. Aurégan, Failure of the Ingard-Myers boundary condition for a lined duct: An experimental investigation, Journal of the Acoustical Society of America 130 (2011) 52-60.